

THE PHYSICAL REVIEW

A journal of experimental and theoretical physics established by E. L. Nichols in 1893

SECOND SERIES, VOL. 105, No. 6

MARCH 15, 1957

Structure of a Shock Front in Argon*

JOHN W. BOND, JR.†

General Electric Company, Missile and Ordnance Systems Department, Philadelphia, Pennsylvania

(Received September 20, 1954; revised manuscript received December 5, 1956)

Steady one-dimensional shocks of such strength that one degree of ionization is of importance are considered. The equation of state of argon is computed, equilibrium conditions behind the shock front are evaluated, and a recombination coefficient derived from detailed balancing. It is shown that for a given shock velocity the shock front is flat and nonluminous at first but soon becomes luminous with corresponding change in hydrodynamic variables and degree of ionization, and that the flat portion decreases in width with increasing shock velocity.

INTRODUCTION

A SHOCK wave traveling through an atmosphere of argon gas may conveniently be described in the following way. In front of the shock wave is the undisturbed atmosphere in equilibrium. Upon being struck by the shock, a violent disturbance occurs, which soon however settles down to a new condition of statistical equilibrium behind the shock. Connection between the two regions of equilibrium is uniquely determined by the Rankine-Hugoniot or shock relations.¹

Disturbance of the statistical equilibrium takes place in the following way. As a shock wave passes through the gas the translational degrees of freedom of the atoms are excited. The distance required to achieve translational equilibrium has been investigated theoretically² and in the limit of strong shocks is of the order of two collision lengths. This seems to have received satisfactory experimental verification.^{3,4} If the temperature of the translational degrees of freedom is sufficiently high, transfer of energy to other degrees of freedom

takes place until complete thermal equilibrium is reached. The region in which this transfer of energy takes place is one of nonequilibrium. The shock front is then defined to be all the region between the undisturbed atmosphere in front of the shock and the point behind the front of the shock at which thermal equilibrium is first essentially achieved.

I. EQUILIBRIUM BEHIND THE SHOCK FRONT

1. Introduction

The general hydrodynamic features of a shock are determined by the properties of the equilibrium regions in front of and behind the shock front. The conditions in front of the shock are completely known, of course. However, the region behind the shock front in argon is a plasma consisting of argon atoms in various states of excitation, argon ions, and electrons. Despite the fact that such a plasma has received considerable attention, particularly at low pressures and temperatures,⁵ knowledge of this state is far from being satisfactory. This is especially true at the high pressures and temperatures behind a shock front.

In Part I, the equilibrium equation of state and the thermodynamic functions of the argon plasma are calculated. There are available several methods for determining the equation of state of gas. Here, the Saha equation has been used and the partition functions

* Most of this work was performed under the auspices of the U. S. Atomic Energy Commission at the Los Alamos Scientific Laboratory, University of California, Los Alamos, New Mexico.

† This report is based on a thesis submitted by the author to the University of New Mexico, 1954 (issued as Los Alamos Report LA-1693), in partial fulfillment of the requirements for the degree of Doctor of Philosophy.

¹ H. A. Bethe and E. Teller, Ballistics Research Laboratory Report No. X-117 (unpublished).

² H. M. Mott-Smith, *Phys. Rev.* **82**, 885 (1951).

³ G. R. Cowan and D. F. Hornig, *J. Chem. Phys.* **18**, 1008 (1950).

⁴ Greene, Cowan, and Hornig, *J. Chem. Phys.* **19**, 427 (1951).

⁵ R. Rompe and M. Steenbeck, *The Plasma State of Gases* (Koppers Company, Inc., Pittsburgh, 1950).

evaluated by a method suggested by Bethe.⁶ The reason for using Bethe's method is that it is simple and well adapted for high-speed computing machines. In this calculation, as indeed throughout this report, it will be assumed that the number of doubly ionized argons is negligible.

2. Equilibrium Conditions

Consider a plasma state behind the shock front in complete thermal equilibrium. Let the concentration $[A]$ be defined as the ratio of the number of neutral argon atoms to the original number before ionization takes place. Similarly $[A^+]$ is the ratio of the number of singly charged argon ions to the original number of argon atoms and $[\mathcal{E}l]$ is the corresponding concentration for electrons, where, at all times

$$[\mathcal{E}l] = [A^+].$$

If g is the average number of particles into which an argon atom splits at temperature T , then

$$g = [A] + 2[A^+], \quad (1)$$

where the factor of 2 is due to the presence of one electron for each ion. Although the density behind a shock front is high, the temperature is also high; hence it seems valid to neglect intermolecular forces and assume the perfect gas equation of state to hold:

$$p = g\rho \frac{R}{M} T, \quad (2)$$

where R is the gas constant per mole and M is the original molecular weight.

Following Bethe, the quantities ϵ and β are defined by the relations

$$E + \frac{p}{\rho} = -T\epsilon = \beta^{-1}, \quad (3)$$

where E is the internal energy per gram.

From (2) and (3),

$$E = (\epsilon - g) \frac{R}{M} T = \left(\frac{\epsilon}{g} - 1 \right) g \frac{R}{M} T,$$

or

$$\beta = \epsilon/g. \quad (4)$$

The quantities β and ϵ have been defined for computational purposes. A parameter analogous to β may be separately defined for atoms, ions, and electrons. This parameter $\beta(q_i)$ will include the energy of translation and electronic excitation; hence for each species

$$\beta(q_i) - 1 = E(q_i)/kT, \quad (5)$$

where $E(q_i)$ is the internal energy per particle and q_i

stands for a particle which may be an argon atom, A , an argon ion, A^+ , or an electron, $\mathcal{E}l$. The quantity ϵ is then given by

$$\epsilon = \beta(A)[A] + \beta(A^+)[A^+] + \frac{I(A)}{kT}[A^+] + \beta(\mathcal{E}l)[\mathcal{E}l].$$

$I(A)$ is the ionization energy for argon and $\beta(A)$ means β for neutral argon and includes the energy of translation and excitation. $\beta(A^+)$ is similarly defined for singly ionized argon. Since for a free particle the energy is $\frac{3}{2}kT$, $\beta(\mathcal{E}l) = 2.5$.

The equilibrium constant for the argon interaction is

$$K = [A^+][\mathcal{E}l]/[A] = x^2/(1-x), \quad (6)$$

where $x = [A^+]$.

3. Partition Functions

Once the equilibrium conditions have been defined, then, for an ionizing reaction the Saha equation may be used to write the equilibrium constant in terms of the partition functions. The Saha equation for the argon equilibrium reaction may be written.

$$K = \left(\frac{2\pi k\mu}{h^2} \right)^{\frac{3}{2}} \frac{1}{n_1 \eta} \frac{T^{\frac{3}{2}} Z(A^+) Z(\mathcal{E}l) e^{-I/kT}}{Z(A)}, \quad (7)$$

where μ is the reduced mass, i.e.,

$$\mu = m^+ m_e / m, \quad m = m^+ + m_e,$$

and n_1 = number of argon atoms in one cm³ of the undisturbed gas in front of the shock, η = density ratio = ρ_4/ρ_1 , ρ_1 = density of the undisturbed gas in front of the shock, ρ_4 = density in the equilibrium region behind the shock, I = first ionization potential of argon, $Z(A^+)$ = internal partition function for the argon ion, $Z(A)$ = internal partition function for the neutral argon atom, and $Z(\mathcal{E}l)$ = internal partition function for the electron.

The density ratio η is used in (7) in place of the corresponding pressure ratio ξ because η varies between 1 and about 10 across the shock front whereas ξ may become very large and, in fact, is set equal to ∞ in the strong-shock approximation.

The internal partition functions are defined by

$$Z = \sum_n g_n e^{-E_n/kT}, \quad (8)$$

with n corresponding to a state of the system with energy E_n and statistical weight g_n (the energy of the ground state is arbitrarily set equal to zero). The internal partition function of the electrons reduces simply to the degeneracy 2. Hence, if

$$f = f(T, \eta) = \left(\frac{2\pi k\mu}{h^2} \right)^{\frac{3}{2}} \frac{1}{n_1 \eta} T^{\frac{3}{2}}, \quad (9)$$

then

$$K = 2f \frac{Z(A^+) e^{-I/kT}}{Z(A)}. \quad (10)$$

⁶H. A. Bethe, Office of Scientific Research and Development Report OSRD 369, 1942 (unpublished).

At high temperatures the higher excited states of the atom become numerous and may contribute appreciably to the partition function. The summing over these higher states could become quite laborious but even worse would be the overlapping of the higher quantum states of neighboring atoms. Therefore, a cutoff must be made. This cutoff successively eliminates the high quantum states of the atom as the density is increased. The corresponding process is termed pressure ionization.

The radius of a hydrogen-like electron orbit is $a_n = a_0 n^2$, where a_0 is the first Bohr radius and n is the principal quantum number. It is now assumed that all electron orbits are suppressed whose radius a_n exceeds half the average distance between neighboring atoms. Let this half-distance be r_0 ; then, if L is the number of atoms per cm^3 in front of the shock,

$$r_0 = \left(\frac{3}{4\pi L \eta} \right)^{\frac{1}{3}}$$

Hence, the limiting value of n is

$$n_\eta = D \eta^{-1/6}, \quad D = \text{const} = \frac{1}{a_0^{\frac{1}{2}}} \left(\frac{3}{4\pi L} \right)^{1/6}$$

As n_η is nonintegral, g is reduced proportionately. For $n \geq n_\eta + \frac{1}{2}$ the state will be completely cut off, and for $n \leq n_\eta - \frac{1}{2}$ the state will be fully counted in the partition function. Hence, the internal partition function of the atom depends not only on the temperature but to a small extent on the density, i.e., $Z = Z(T, \eta)$.

In the above approximation the partition function of the free electrons is underestimated since their potential energy is neglected. Also, the integration over phase space is not carried out properly. While it is difficult to estimate the size of the error, it cannot be large since theory and experiment are in good agreement (see Fig. 8 and paper of Shreffler and Christian⁷). In addition, the above theory agrees with more precise calculations made at Los Alamos.

The contribution to the partition function from the low states is easy to obtain because of their small number. However, the contributions from the higher states which have one electron excited to $n \geq 4$ is a different matter both because of the great number available and because of the cutoff that must be made. Hence, the partition function for the neutral atom may be written as

$$Z = Z_{\text{low}} + Z_{\text{high}}, \quad (11)$$

where Z_{low} is summed over the low states ($n=3$) as in (8).

The ground state of argon is a $(3p)^6 1S_0$ level with a multiplicity of one and an energy by convention equal to zero. There is also a level from the configuration $(3p)^5 (3d)$, observed spectroscopically, which has a

relatively high energy, *viz.*, 113 000 cm^{-1} or 162 500 degrees. The level has a multiplicity 60. Levels with two excited electrons have such high energies as to be unimportant in the partition function.

The quantity Z_{high} may be evaluated by the following approximation: Consider a highly excited atom as an ion with an electron moving around the ion in a large orbit. The spectrum will be alkali-like and the energy E_{nl} , of a state of principal quantum number n and orbital quantum number l , will be

$$E_{nl} = I + E_{\text{ion}} - E_{nl}', \quad (12)$$

where E_{ion} = excitation energy of the ion (≥ 0), and E_{nl}' = binding energy of the electron.

If (12) is substituted in (8), Z_{high} becomes

$$Z_{\text{high}} = Z_{\text{ion}} e^{-I/kT} z_{\text{high}}, \quad (13)$$

Z_{ion} is determined similarly to Z_{low} although the low states are more numerous for A II than for A I. The quantity z_{high} is the partition function for the (one-electron) high excited states of the neutral argon atom, when one neglects the multiplicity of the core configuration (which is included of course in Z_{ion}). It is given by

$$z_{\text{high}} = \sum g_{nl}(\eta) e^{+E_{nl}'/kT}, \quad (14)$$

where $g_{nl}(\eta)$ is the adjusted multiplicity. As shown by (12), E_{nl}' corresponds to a positive binding energy which is subtracted from the energy of the ion, i.e., $E_{nl}' = I - E_n$ with E_n the excitation energy. The high excited states of the ion have not been included because their contribution to the partition function is negligible in the temperature range concerned.

4. Energy Content

If the partition function is known, it is possible to obtain the various other thermodynamic functions. The energy content is of particular interest because of its importance in determining the shock conditions (Sec. 5).

The average energy per particle in units of kT is

$$\beta(q_i) - 1 = \frac{3}{2} + \frac{\sum g_n(E_n/kT) e^{-E_n/kT}}{Z}. \quad (15)$$

The $\frac{3}{2}$ represents translational energy, E_n the internal energy per particle for the remaining degrees of freedom, and Z is the corresponding partition function.

Let

$$W = \sum g_n(E_n/kT) e^{-E_n/kT}; \quad (16)$$

then

$$\beta = (5/2) + (W/Z).$$

W may be evaluated in the same way as Z , i.e.,

$$W = W_{\text{low}} + W_{\text{high}},$$

with W_{low} given by (16) but summed over just the low states.

⁷ R. G. Shreffler and R. H. Christian, J. Appl. Phys. 25, 324 (1954).

5. Shock Front without Heat Conduction or Viscosity

In Secs. 2 to 4 it has been shown how component concentrations and energy content may be calculated in a gas which is in a state of complete thermal equilibrium. If this equilibrium state is specified to be that which exists behind a shock front, then the density and temperature are determined by the conservation equations, the equation of state, the shock velocity, and the initial conditions. It is assumed that heat conductivity and viscosity can be neglected which is perfectly valid if the conditions are those of equilibrium and there are no dissipative losses.

Consider a one-dimensional shock for which the shock equations may be written as follows:

Conservation of mass:

$$\rho v = m = \text{const}, \quad (17)$$

where ρ is the density and v the velocity with respect to the shock front, i.e.,

$$v = u - U, \quad (18)$$

u being the material velocity and U the shock velocity.

Conservation of momentum:

$$p + mv = mV_0, \quad V_0 = \text{const}. \quad (19)$$

Conservation of energy:

$$\beta p / \rho + \frac{1}{2}v^2 = \frac{1}{2}C^2, \quad C = \text{const}. \quad (20)$$

If (17) and (2) are substituted into (19) and (20), then, after dividing through by ρ_1^2 , the functions F_1 and F_2 are obtained:

$$F_1 = g\eta^2(R/M)T - UV_0\eta + U^2, \quad (21)$$

and

$$F_2 = \beta g(R/M)\eta^2T - \frac{1}{2}C^2\eta^2 + \frac{1}{2}U^2, \quad (22)$$

where F_1 and F_2 must go to zero together.

The constants V_0 and C are determined from the conditions in front of the shock; hence, for a given value of U , and if $\beta(\eta, T)$ and $g(\eta, T)$ are known, the quantities η , T , ξ , and u may be uniquely determined in the shock front and behind the shock front.

In the above equation radiation has been neglected but a brief consideration shows that this is probably a good approximation for the range of shock strengths⁸ under consideration. For example, if $\xi = 500$, $\eta = 7$, and $\gamma = 4/3$ which is about right for $T = 20\,000$ degrees and $U = 6 \times 10^5$ cm/sec, then the energy density for internal degrees of freedom is 10^{11} ergs per gram. However, if black-body radiation is assumed, the radiation density is only about 10^5 ergs per gram.

Assuming about 0.1 of the argon atoms are either excited or ionized and an average wavelength for emitted radiation of 2×10^{-5} cm, a rate of radiation of about 10^{15} ergs per gram per second is obtained. If this is

compared with the internal energy, *viz.*, 10^{11} ergs per gram it is seen that the relaxation time, E/\dot{E} , for radiation loss is of the order of $100 \mu\text{sec}$ which is much longer than the time for complete relaxation of the shock front. (As will be shown in Part II, this time is of the order of 10^{-8} sec, which is also about the lifetime of a radiative transition.)

Computations for Parts I and II of this report have been given in both tabular and graphical form.⁹ The equation of state for argon has been tabulated in terms of the partition functions and the equilibrium constant for temperatures between 7500°K and $26\,000^\circ\text{K}$ and density ratios between 1 and 20. The equilibrium region behind the shock front has been computed for shock velocities between 3 and 9 times 10^5 cm/sec and for two fore-pressures, $p_1 = 59.3$ cm Hg and $p_1 = 1.0$ cm Hg (see Figs. 8 and 9).

II. NONEQUILIBRIUM REGION

1. Introduction

In Part I it has been shown how the conditions in the region behind the shock where thermal equilibrium is assumed to be established may be completely determined. The nonequilibrium portion of the shock, i.e., the part between the undisturbed gas in front of the shock and the equilibrated region behind the shock, will now be examined.

Although a true thermodynamic temperature does not exist in this region, the velocity distribution of the neutral atoms, the ions, and the electrons is at each point close to Maxwellian. A local "temperature" which is characteristic of this distribution may therefore be introduced. The use of such a temperature is probably valid, since the high density and pressure involved cause a Maxwellian distribution to be very quickly established.

The flow region involving the shock front may be conveniently divided into four parts (see Fig. 1). The undisturbed gas in front of the shock is region 1. Region 2 represents that part of the shock front in

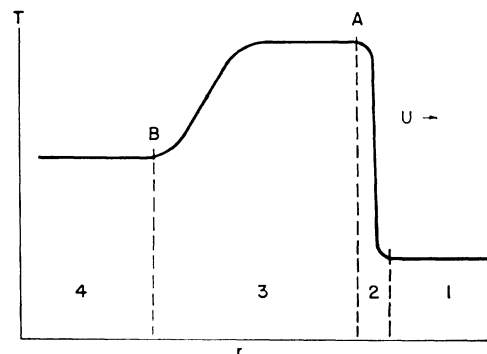


FIG. 1. Temperature vs distance in a steady shock front, showing the equilibrium and nonequilibrium regions.

⁸ Shock strength is defined here as the pressure ratio $\xi = p_4/p_1$, where p_4 is the equilibrium pressure and p_1 is the fore-pressure.

⁹ J. W. Bond, Jr., Los Alamos Report LA-1693, 1954 (unpublished).

which translational equilibrium takes place which, for strong shocks, has a width of about two mean free paths. In region 3 equilibrium of the various internal degrees of freedom of the gas atoms takes place, and in region 4 it is assumed that complete thermodynamic equilibrium again exists. In Fig. 1 equilibration between translational degrees of freedom is first reached at point *A* and complete equilibration between all degrees of freedom is first reached at point *B*.

To obtain the conditions at point *A*, the shock equations may be used, with the assumption, however, that the internal degrees of freedom are not excited. Hence, a constant γ , *viz.*, $\gamma=5/3$ for argon, is used. The pressure at point *A* is given by

$$\frac{p_A}{p_1} = \xi_A = \frac{2\rho_1}{\rho_1(\gamma+1)} U^2 - \frac{1}{\eta_\infty},$$

and the density from

$$\frac{\rho_A}{\rho_1} = \eta_A = \frac{\eta_\infty \xi_A + 1}{\xi_A + \eta_\infty}, \quad \eta_\infty = \frac{\gamma+1}{\gamma-1}.$$

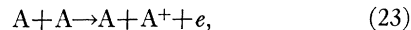
The temperature ratio is given by

$$T_A/T_1 = \xi_A/\eta_A.$$

2. Production of Electrons in the Shock Front

If the cross sections for all the various atomic interactions that take place in a shock front were known, it would be possible to compute the rate of transfer of energy from the translational degrees of freedom to the other degrees of freedom, *i.e.*, the rate at which true thermal equilibrium is established. For argon a relatively simple model of the shock front will be adopted which involves only cross sections that either have been determined experimentally or may be computed.

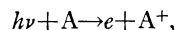
There are numerous processes by which electrons are produced in forming a plasma; however, a brief consideration shows that to a fair approximation all but two may be neglected, *viz.*,



and



Reactions involving the production of multiply-ionized atoms may be neglected because of the higher ionization potentials. The reaction $A + A^+ \rightarrow 2A^+ + e$ is neglected because, while its cross section is about the same as for (23), the concentration of A^+ is relatively small. The absorption reaction,



is neglected because of the long lifetime involved, the low radiation density (see Part I, Sec. 5), and because the photons escape from the system.

Finally, the argon atom may be excited by processes similar to the ones listed above. Once excited it can drop into a metastable state from which ionization can

take place either by collisions or by a photoprocess. In both cases radiative transitions are involved and, as pointed out above, the lifetimes of radiative transitions are of such lengths as to warrant neglect of excitation. It is possible, however, that excitation processes compete with some of the one-step processes, but the cross sections are not known very well.¹⁰

Since, at the peak of the shock (point *A*, Fig. 1), only the translational degrees of freedom are excited and there are no electrons present, the reactions between argon atoms will be considered first. The production term may be written

$$q_1 = \int \int f(v_1) f(v_2) \sigma_i(v_r) v_r d\mathbf{v}_1 d\mathbf{v}_2, \quad (25)$$

where $f(v_1)$, $f(v_2)$ are the normalized Maxwellian distributions for the two reactants (in this case, neutral argon atoms), $\sigma_i(v_r)$ is the ionization cross section, v_r is the relative velocity, and $d\mathbf{v}_1$, $d\mathbf{v}_2$ are the elements of volume in velocity space. The use of Maxwellian distributions here is particularly good because of the high shock velocities to be considered¹¹ and because the masses of the reactants are equal.

The ionization cross section for reaction (23) was measured by Rostagni¹² for various low values of the relative energy. In the very low energy range, say below 100 ev, the measurement of the cross section is particularly difficult because the chance of energy transfer is so minute that it is not easy to reduce background effects to an unimportant magnitude. Wayland¹³ found a low-energy tail with a threshold value of 48 ev which has been fitted to the Rostagni results.

When one inserts the expressions for the distribution functions into (25), the following relation for q_1 is obtained:

$$q_1 = A \int \int \exp\left(-\frac{mv_1^2}{2kT}\right) \exp\left(-\frac{mv_2^2}{2kT}\right) \times \sigma(v) v d\mathbf{v}_1 d\mathbf{v}_2. \quad (26)$$

A is the normalizing factor which is given by

$$A = \frac{n^2}{2} \left(\frac{m}{2\pi kT}\right)^3,$$

where n is the number density of argon atoms at an arbitrary point in the shock front. If the production coefficient is

$$\beta_1(T) = \frac{1}{2} \left(\frac{m}{2\pi kT}\right)^3 \int \int \exp\left(-\frac{mv_1^2}{2kT}\right) \exp\left(-\frac{mv_2^2}{2kT}\right) \times \sigma(v) v d\mathbf{v}_1 d\mathbf{v}_2,$$

¹⁰ H. Maier-Leibnitz, Z. Physik **95**, 499 (1935).

¹¹ H. K. Sen, Phys. Rev. **92**, 861 (1953).

¹² A. Rostagni, Nuovo cimento **13**, 389 (1936).

¹³ H. Wayland, Phys. Rev. **52**, 31 (1937).

then the production of electrons by reaction (23) is given by $q_1 = \beta_1 n^2$.

Once electrons have been produced by the $A+A$ reaction, then reactions between electrons and atoms take place. It has been assumed that ionizing reaction (24) is the only one of importance; the corresponding production term is $q_3 = \beta_3 n n_e$, where β_3 is similar in form to β_1 except that the masses and temperatures of the two colliding particles differ. The cross section σ_3 is the cross section for the reaction (24). The values used were those measured by Bleakney¹⁴ to which were fitted the low-energy tail measured by Stevenson and Hipple.¹⁵

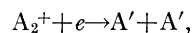
Implicit in the use of β_3 in the above form is the assumption that the electrons are in a Maxwellian velocity distribution. This assumption is probably valid if electron-electron collisions are predominant, and such is the case if the degree of ionization x is greater than about 10^{-3} . Hence, if $x > 10^{-3}$ it is assumed that the electrons are at a temperature T_e and the plasma at a temperature T . In this range, and before equilibrium is reached, the electron temperature is somewhat lower than the plasma temperature because each time reaction (24) occurs an amount of kinetic energy equal to the ionization energy of argon is lost to the electrons. The rate of decrease of electron energy due to ionization collisions is offset by the rate of increase in electron energy due to Coulomb collisions. A formulation for the latter rate is given by Landau.¹⁶

3. Recombination Processes

After electrons have been produced in quantity, recombination between the electrons and argon ions becomes important. There appear to be no experimental measurements of the recombination coefficient in the temperature and density range for the shocks under consideration. Therefore, the recombination processes that could occur will be discussed separately.

Dielectronic recombination involves the formation of a doubly excited atom, i.e., $A^+ + e \rightarrow A''$, which then either reverts to its initial state, ejecting one electron and leaving the other excited electron in a bound state, or undergoes a radiative transition going over to a stable, singly excited state. A computation by Massey and Bates¹⁷ shows that this process may be neglected here.

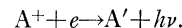
An argon atom and an argon ion may unite in a triple impact to form a molecular ion, A_2^+ . Because of the short duration of the time of formation, the dissociative recombination process,



could be of considerable importance. However, molec-

ular binding energies of this type are much lower than the mean temperatures which are in the range from 2 to 3 electron volts; hence, it is probably safe to assume that the concentration of A_2^+ is negligibly small.

Radiative capture of an electron by an argon ion is a two-body process and may be represented by the reaction



Here again experimental cross sections are not available, and hence theoretical values must be used. A classical theory for radiative recombination due to Kramers¹⁸ will be considered first.

Behind the front of the shock a plasma is formed which consists of free electrons and neutral and singly-ionized argon atoms in various states of excitation with respective concentrations n_e , n , and n^+ , where $n^+ = n_e$, and the velocity distributions are Maxwellian. The radiative capture cross section for an electron by an argon ion may then be estimated in the following way. When an electron passes through an electric field in which the charge distribution is uniform, it loses energy at a rate dependent upon the square of the acceleration. If the accelerating force is exerted by a positive charge, the path of the electron will be hyperbolic and such that the greatest acceleration, and consequently the greatest energy loss, will be at the point of closest approach to the positive charge. Let us assume each argon nucleus to be surrounded by a uniform charge distribution, which may be obtained by taking the self-consistent field calculations of Hartree¹⁹ for a neutral argon atom and reducing the outer orbital charge by unity with appropriate adjustment of the radius and charge density. When the electron penetrates this charge distribution it radiates energy; and if the assumption is made that when the energy loss is greater than the initial kinetic energy of the electron, capture takes place, then the cross section is

$$\sigma(v) = 1.4885 \times 10^5 Z_e^{8/5} / V^{14/5},$$

in agreement with a formula given by Biondi.²⁰ In this formula the dependence of the effective charge Z_e on the velocity v is not included. However, even if this is done it is found that $\sigma(v)$ is far too large.

If instead of using the above classical theory, quantum theory is used, more satisfactory results are obtained. Usually the cross section σ_{ph} for the inverse process, that is, photoelectric absorption, is calculated. This causes but little difficulty, for the radiative capture cross section σ_r can be obtained from it by detailed balancing.

It is possible to use a rather simple approximation for the photoelectric cross section since the processes involved are those in which the kinetic energy of the

¹⁴ W. Bleakney, Phys. Rev. **36**, 1303 (1930).

¹⁵ D. P. Stevenson and J. A. Hipple, Phys. Rev. **62**, 237 (1942).

¹⁶ L. Landau, Physik. Z. Sowjetunion **10**, 154 (1936).

¹⁷ H. S. W. Massey and D. R. Bates, Repts. Progr. Phys. **11**, 62 (1942).

¹⁸ H. A. Kramers, Phil. Mag. **46**, 836 (1923).

¹⁹ D. R. Hartree and W. Hartree, Proc. Roy. Soc. (London) **A166**, 450 (1938).

²⁰ M. A. Biondi and S. C. Brown, Phys. Rev. **76**, 1697 (1949).

electron in the ionized state is small compared to the ionization energy. For this case it is valid to expand the continuum wave function occurring in the matrix elements of the transition probability about the function for zero energy. If a similar expansion (which is *a priori* much less justified, but which nevertheless gives good numerical results) is used for the bound-state wave functions, and the resulting cross section averaged over all values of the orbital angular momentum of the bound state, the cross section derived by Menzel and Pekeris²¹ and discussed by Mayer²² is obtained.

With appropriate modifications for argon and assuming hydrogenic wave functions for the higher excited states and an effective charge of 5 for the 3*p* orbital, the total capture cross section is given by

$$\sigma_r = 3.018 \times 10^{-21} / E \text{ cm}^2,$$

with *E* in electron volts. This formula agrees well with values for argon obtained by adjusting Bates' results on hydrogen and oxygen.²³

The radiative recombination coefficient is given by

$$\alpha_3 = \left(\frac{2}{\pi}\right)^{\frac{1}{2}} \left(\frac{\mu}{kT}\right)^{\frac{3}{2}} \int_0^\infty \exp\left(-\frac{\mu v^2}{2kT}\right) \sigma_r(v) v^3 dv,$$

or

$$\alpha_3 = 2.174 \times 10^{-11} / T^{\frac{1}{2}}. \quad (27)$$

Finally, consider three-body recombination. If Thomson's²⁴ theory is used, one may compute the chance that an electron, after colliding with a neutral argon atom, is captured into an orbit about a neighboring ion which must be at a distance less than $r_0 = 2e^2/3kT$. The resulting cross section is approximately

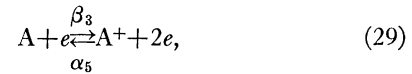
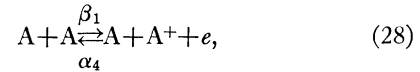
$$\sigma_{th} = \frac{8\pi r_0^3 m_e n \sigma_d}{m},$$

where m_e is the mass of an electron, m the mass of an argon atom, and σ_d the diffusion cross section for electrons in argon.

Since σ_r and σ_{th} are of the same order of magnitude, it would be necessary to take both the radiative and three-body recombination processes into account. However, in the temperature range 1 to 3 eV the Thomson theory is only applicable for atom densities $10^{22} \lesssim n \lesssim 10^{24}$ per cm³ whereas the atom densities achieved in the shocks being treated lie in the range 10^{18} to 10^{20} per cm³.

In view of the inapplicability of the Thomson theory, another method aimed at finding the recombination coefficient α must be used. To obtain such a method consider the derivation of the source term. It has been

assumed that the only significant reactions occurring in the plasma, which consists of argon atoms A, argon ions A⁺, and electrons *e*, are the following:



The electron production rates are given by the β 's and the recombination rates by the α 's. From these reactions a source term may be written as

$$S = dn_e/dt = \beta_1 n^2 + \beta_3 n n_e + \beta_9 n n_\nu - \alpha_4' n m_e^2 - \alpha_5' n_e^3 - \alpha_3 n_e^2, \quad (31)$$

where all the coefficients are functions of temperature only, and where $\alpha_4' = \alpha_4/n$ and $\alpha_5' = \alpha_5/n_e$. The atom density is n , electron density n_e , photon density n_ν , and electron and ion densities are equal. The recombination coefficient may then be written

$$\alpha = \alpha_4' n + \alpha_5' n_e + \alpha_3. \quad (32)$$

In the equilibrium state $dn_e/dt = 0$ or, from (31), if one uses the asterisk to denote equilibrium values,

$$\alpha^* = \alpha_4' n^* + \alpha_5' n_e^* + \alpha_3 = \frac{n^{*2}}{n_e^{*2}} \left(\beta_1 + \beta_3 \frac{n_e^*}{n^*} + \beta_9 \frac{n_\nu^*}{n^*} \right).$$

From Part I,

$$n^*/n_e^* = (1-x)/x;$$

hence

$$\alpha^* = \alpha_4' n^* + \alpha_5' n_e^* + \alpha_3 = \beta_1 \left(\frac{1-x}{x}\right)^2 + \beta_3 \left(\frac{1-x}{x}\right) + \beta_9 \frac{n_\nu^*}{n^*} \left(\frac{1-x}{x}\right)^2. \quad (33)$$

By the principle of microscopic reversibility, not only must the over-all production of electrons be zero in the equilibrium state, but each individual reaction (28) to (30) must be balanced. Hence

$$\alpha_4' = \frac{1}{n^*} \beta_1 \left(\frac{1-x}{x}\right)^2,$$

$$\alpha_5' = \frac{1}{n_e^*} \beta_3 \left(\frac{1-x}{x}\right),$$

$$\alpha_3 = \frac{n_\nu^*}{n^*} \beta_9 \left(\frac{1-x}{x}\right)^2.$$

Thus the nonequilibrium recombination rate α of (32) may be obtained from knowledge of the equilibrium

²¹ D. H. Menzel and C. L. Pekeris, Monthly Notices Roy. Astron. Soc. **96**, 77 (1935).

²² H. Mayer, Los Alamos Report LA-647 (unpublished).

²³ Bates, Buckingham, Massey, and Unwin, Proc. Roy. Soc. (London) **A170**, 322 (1939).

²⁴ H. S. W. Massey and E. H. S. Burhop, *Electronic and Ionic Impact Phenomena* (The Clarendon Press, Oxford, 1952).

concentrations and β_1 and β_3 (giving α_4' and α_5') and from the quantum formula for radiative recombination (giving α_3), i.e.,

$$\alpha = \frac{n}{n^*} \beta_1 \left(\frac{1-x}{x} \right)^2 + \frac{n_e}{n_e^*} \beta_3 \left(\frac{1-x}{x} \right) + \alpha_3. \quad (34)$$

4. Structure of the Shock Front

The equation for the rate of electron production, i.e., the source term, is given by Eq. (31). In order to apply this equation to the nonequilibrium part of the shock front, a term that expresses the change in macroscopic density must be incorporated. This may be done by writing the continuity equation in terms of electron density as

$$\partial n_e / \partial t + \partial (u n_e) / \partial X = S,$$

where u is material velocity and X is the Eulerian distance coordinate.

In a Lagrangian system where x' is the distance coordinate, this becomes

$$\left. \frac{dn_e}{dt} = \frac{\partial n_e}{\partial t} \right]_{x'} = S - n_e \frac{\rho}{\rho_1} \frac{\partial u}{\partial x'};$$

and substituting

$$\rho_1 \partial V / \partial t = \partial u / \partial x', \quad V = 1/\rho,$$

the following equation is obtained:

$$d \log(n_e V) / dt = S / n_e. \quad (35)$$

The density of the plasma is given by $\rho = m(n + n_e)$; and since the degree of ionization x is

$$x = n_e / (n + n_e),$$

it follows that $n_e V = x/m$. Thus (35) becomes, when one uses (31),

$$\begin{aligned} \frac{dx}{dt} = & \frac{\beta_1}{mV} + \frac{x}{mV} (\beta_3 - 2\beta_1) + \frac{x^2}{mV} \left(\beta_1 - \beta_3 - \alpha_3 - \frac{\alpha_4'}{mV} \right) \\ & + \frac{x^3}{m^2 V^2} (\alpha_4' - \alpha_5'), \end{aligned} \quad (36)$$

where it is assumed that the photon density n_ν is negligible.

The various production and recombination coefficients are all temperature-dependent and, in general, may depend on both the plasma and electron temperatures. In the initial phase of the shock front the most significant reaction is that going to the right in (28), and the corresponding production coefficient β_1 depends only on the plasma temperature. When a sufficient number of electrons are produced by reaction (28), the reaction going to the right in (29) becomes important and the production coefficient β_3 depends

primarily on the electron temperature T_e . As equilibrium is approached, the various recombination processes as well as the photoelectric process become important; but in the region close to equilibrium the electron temperature is not much different from the plasma temperature and α_4 , α_5 , α_3 , and β_9 may all be assumed to depend on the plasma temperature T .

If the electron temperature has a significant effect on the structure of the shock front, it becomes important to determine its value. In order to do this, an additional relation involving T_e is needed. Such a relation may be found from an energy balance between processes in which electrons lose energy and those in which electrons gain energy. In the region of the shock front in which T_e plays an important part, it has already been noted that the electrons lose energy by the ionizing process (29) and gain energy by Coulomb collisions. The

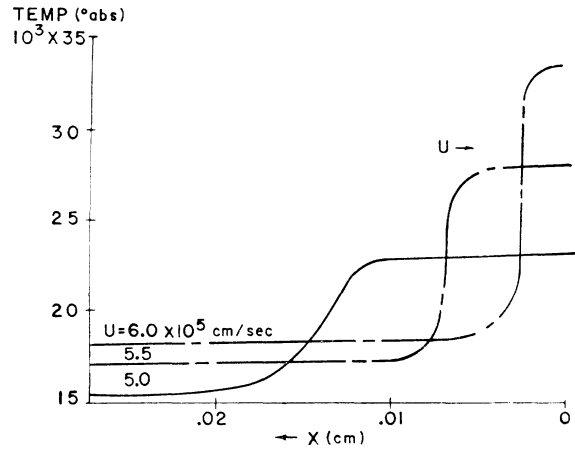


FIG. 2. Temperature vs (Eulerian) distance in the shock front for various shock velocities ($p_1 = 59.3$ cm Hg).

resulting energy balance is given by

$$\omega = \frac{3}{2} k n_e \frac{dT_e}{dt} - I \frac{dn_e}{dt},$$

where I is the ionization potential. Inserting the Landau¹⁶ relation for dT_e/dt and the proper reaction rate for dn_e/dt , we have for ω ,

$$\begin{aligned} \omega = & - \frac{n_e^2 e^A}{m_A} \left(\frac{8\pi m_e}{kT_e} \right)^{\frac{1}{2}} \left(1 - \frac{T}{T_e} \right) \log \left[\frac{(kT_e)^2}{n_e e^6} \right] \\ & - I n_e n_A \left(\frac{2}{\pi k^3} \right)^{\frac{1}{2}} \left(\frac{\alpha_e \alpha_A}{\alpha} \right)^{\frac{1}{2}} \int \exp \left(- \frac{\alpha_e \alpha_A}{2k\alpha} v^2 \right) \sigma(v) v^3 dv. \end{aligned}$$

In this relation

$$\alpha_e = m_e / T_e, \quad \alpha_A = m_A / T_A, \quad \alpha = \alpha_e + \alpha_A.$$

In computing the electron temperature from ω , the varying plasma properties in the shock front must be considered. Thus ω is a source term similar to S and

the equation used is

$$\frac{\partial E_e}{\partial t} + \frac{\partial}{\partial X} [u(E_e + p_e)] = \omega,$$

where E_e is the electron energy per unit volume and p_e is the electron pressure. This equation must be coupled with the three conservation equations, the equation of state, and the equation of continuity for electrons. The state variables then are ρ , T , n_e , T_e and the coordinate variables are X and t .

The equations were integrated across an argon shock front for three different shock velocities, viz., $U = 6.0, 5.5,$ and 5.0×10^5 cm/sec, and for a fore-pressure of 59.3 cm Hg and temperature of 285°K (corresponding to atmospheric conditions at Los Alamos). It was assumed that Maxwellian distributions prevailed at all times; hence the equations given in Part I were used

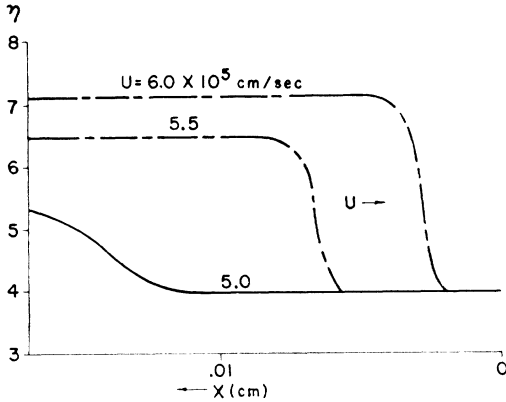


FIG. 3. Compression η vs (Eulerian) distance in the shock front for various shock velocities ($p_1 = 59.3$ cm Hg).

to obtain the various hydrodynamic quantities. In order to shorten the computations, the following relation for ϵ was used:

$$\epsilon = 2.5 + x(5.5 + 183\,000/T).$$

This involves the assumptions that $\beta(A^+) = 2.5$ and that

$$x = \frac{W}{Z} / \left(3 + \frac{W}{Z} - \frac{W_{ion}}{Z_{ion}} \right),$$

both of which are good approximations for the range of shock velocities considered. The results of the integration are shown in Figs. 2 to 7.

It has been noted previously that the electron temperature is lower than the plasma temperature. This has the effect of delaying the time at which reactions (28) and (29) produce electrons at equal rates. The point where these rates are equal is called the *onset point* and can be determined by equating the first two terms on the right of Eq. (36).

The shock front may now be described in the following way. When a shock front passes a point X the

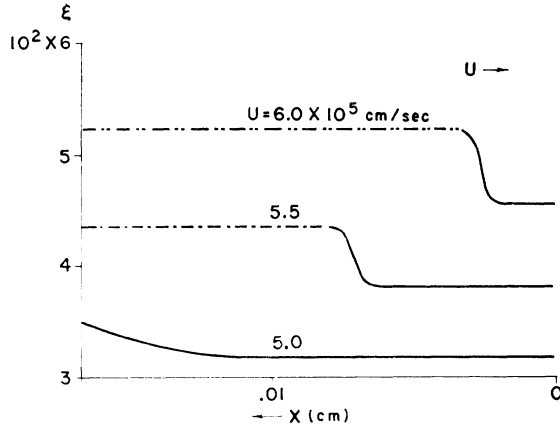


FIG. 4. Pressure ratio ϵ vs (Eulerian) distance in the shock front for various shock velocities ($p_1 = 59.3$ cm Hg).

translational degrees of freedom of the gas are first excited and translational equilibrium is achieved within about two collisions. This point is referred to here as the peak of the shock. The time required for translational equilibrium is small compared to that for the remaining processes involved in the shock front and hence is not included in the computations. The local temperature at the peak of the shock is high enough so that a significant amount of energy may be transferred from the translational degrees of freedom to those of electronic excitation and ionization. This is clearly indicated in Fig. 2 where it is seen that the equilibrium temperature T^* is considerably lower than T_A at the peak of the shock. This is particularly true for increasing shock velocity as shown in Table I:

The only reactions available at first are collisions between argon atoms for which the corresponding ionization cross section is quite small. This means that the transfer of energy takes place rather slowly until *onset of ionization* is reached (see Fig. 6). Thus the values at the peak of the shock remain approximately

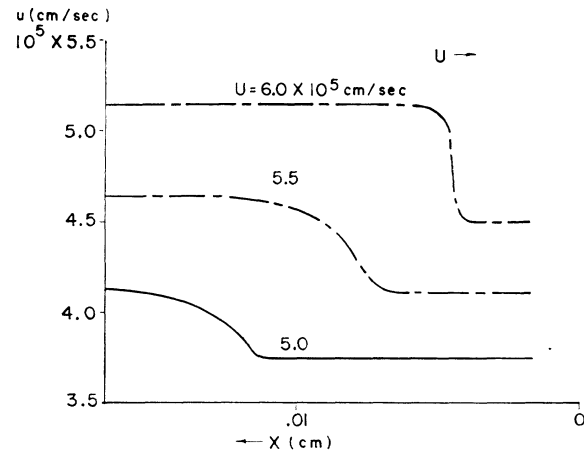


FIG. 5. Material velocity u vs (Eulerian) distance in the shock front for various shock velocities ($p_1 = 59.3$ cm Hg).

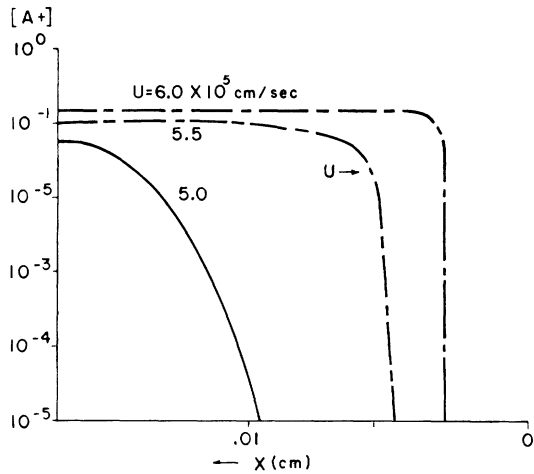


FIG. 6. Ionization vs (Eulerian) distance in the shock front for various shock velocities ($p_1=59.3$ cm Hg).

unchanged for some distance, resulting in a rather flat region in the shock front. This is true for all shock parameters as Figs. 2 to 7 show. This distance is referred to as the *onset width*. If the relaxation point is that point at which 63% of the equilibrium ionization is achieved, it may be seen that the onset width offers the most important contribution to the total relaxation width. By considering the leading term in Eq. (36), it is seen that the onset width scales inversely with initial density ρ_1 (or pressure p_1) at constant initial temperature T_1 .

In determining the onset width, β_1 is the most significant quantity because the degree of ionization is small in this region. If β_1 is correctly evaluated, the onset width will depend on the electron temperature. Landau's theory¹⁶ shows that the velocity at which the electron temperature approaches the ion temperature is approximately proportional to the ion density and inversely proportional to the electron temperature. Hence, for a low degree of ionization, the velocity of equilibration is low, which means that the onset width may be somewhat greater than if the electron and plasma temperatures were equal. As the ionization increases, the velocity of equilibration increases in such a way that for an ion density greater than 10^{18} per cm^3 and for an electron temperature of 2 eV it is probable that the electron and ion temperatures are about the same.

Once the onset of ionization is reached, transfer of energy from translational degrees of freedom to elec-

TABLE I. Temperature in an argon shock front; $p_1=59.3$ cm Hg.

M_s (shock Mach numbers)	U (cm per sec)	T_A/T^*
17.4	5.0×10^5	1.46
19.1	5.5×10^5	1.60
20.8	6.0×10^5	1.78

tronic excitation and ionization proceeds quite rapidly. This results in a more rapid change in the shock parameters, especially the temperature (Fig. 2) and the degree of ionization (Fig. 6). Again it is seen that the effect is more violent for higher shock velocities; e.g., if the distance in which this sudden change takes place is ΔX , then for $U=6 \times 10^5$ cm per sec, $\Delta X \approx 0.01$ cm, while for $U=5 \times 10^5$ cm per sec, $\Delta X \approx 0.04$ cm. At first the electron production term involving β_3 is most important, but soon the recombination terms take over and equilibrium is quickly achieved. The shape (or profile) of this region is rather sensitive to the value of α , but because the region is relatively narrow α does not have much effect on determining the total relaxation width of the shock front.

It is interesting to note that there is a range of shock velocities in which the width of the shock front may be significant, i.e., in which the conditions in the shock front are considerably different from the equilibrium

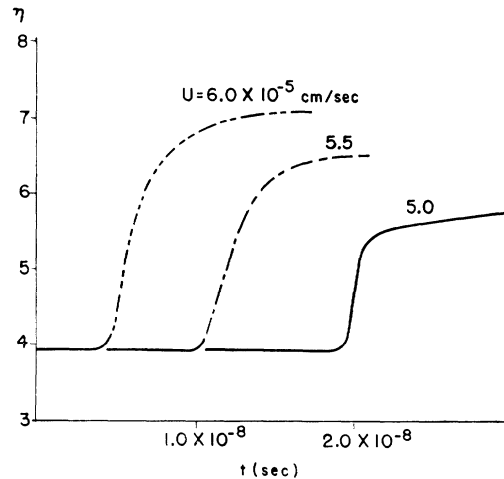


FIG. 7. Compression in the shock front vs time ($p_1=59.3$ cm Hg).

conditions behind the shock front. At low shock velocities, i.e., below about 3×10^5 cm/sec, there is not much ionization behind the shock front, hence γ remains constant and the conditions at the peak of the shock remain unchanged. As the shock velocity U increases above 3×10^5 cm/sec, γ decreases and a long and relatively low temperature bump appears behind the head of the shock. (This is an indentation in terms of pressure and density.) As U becomes greater the bump becomes progressively higher but shorter until at 10^6 cm/sec it extrapolates to a thickness of approximately 10^{-6} cm with a peak temperature of about $90\,000^\circ\text{K}$, and an equilibrium temperature of about $26\,000^\circ\text{K}$. (However, for $U \sim 10^6$ cm/sec, the number of doubly ionized atoms can no longer be neglected.) This picture of the shock front is qualitatively the same if the fore-pressure is 1.0 cm Hg.

In the above calculations, second order effects have been neglected. For example, if the transport properties

of the gas are considered, it is found that there is a small resultant diffusion of the electrons toward the front of the shock (see under *Electric effects*, Sec. 6 below), although the magnitude of the process is such that the macroscopic properties of the gas remain unaffected. Also, the effect of radiation streaming ahead of the shock is probably unimportant since the energy loss by radiation is relatively small as is the density of radiant energy (Part I, Sec. 5).

5. Effect of Impurities

Impurities such as oxygen or other molecules in the argon would have a strong influence on two parts of the computation. In the case of the equilibrium calculation the additional degrees of freedom, i.e., rotation, vibration, dissociation, and molecular excitation, because of their lower energy levels, will soak up a considerable amount of energy which is then not available for exciting (or ionizing) the argon atom. Calculations show that a small percentage (between about 1 and 10%) of oxygen in the argon may keep the argon from ionizing.

The second place in which impurities play an important part is in the determination of the onset of ionization. If the ionization cross-section between argon and O_2 or O is large, then even though the amount of oxygen is small, enough electrons may be furnished for the $A+e$ reaction to take over, resulting in an effective decrease in the onset width.

6. Comparison with Experiment

In general, experimental work is quite meager although this field is now being explored, particularly by A. R. Kantrowitz and his co-workers, by O. Laporte, and by various people at Los Alamos. As mentioned previously, the shock velocity is the one well-determined quantity for a shock wave; and, of course, it may be assumed that the conditions in front of the shock are known.

Material velocity.—Shreffler, Christian, and others have measured the material velocity in a shock wave immediately behind the shock front.⁷ Their measurements correspond to the velocity in the equilibrium region and are plotted in Fig. 8 along with the theoretical values. It is seen that experiment and theory are in good agreement in this region.

Electric effects.—Unpublished measurements at Los Alamos have shown that inside the shock front there exists a positive potential, the magnitude of which increases with increasing shock strength. Also, for a given shock velocity the potential is much smaller if the gas is diatomic. This latter effect, as explained in Sec. 5, is due to the presence of the additional degrees of freedom in the diatomic gas which absorb energy that otherwise would have gone into exciting or ionizing the atom.

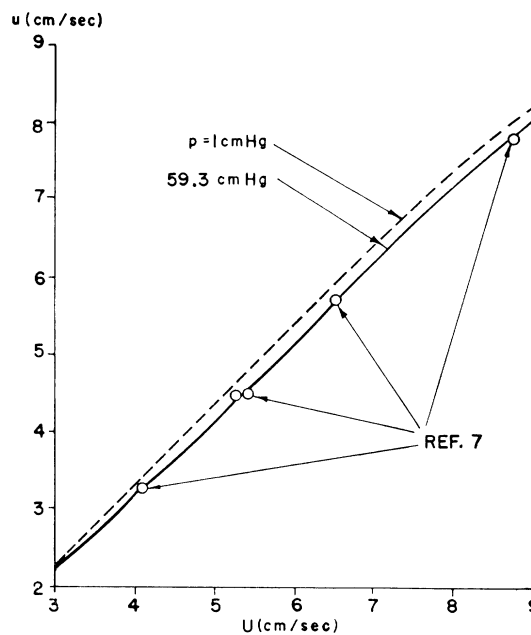


FIG. 8. Material velocity vs shock velocity in the equilibrium region behind the shock front.

Cowling²⁵ has shown that diffusion can be more important than viscosity or thermal conductivity in its effect on shock propagation, particularly if the gas is composed of two constituents having a large mass difference and if the pressure gradient is large, the direction being such that the heavier particles tend to move toward the regions of greater pressure. In the present case such a situation exists immediately in front of the equilibrium region (see Figs. 4 and 6). Hence, a separation of ions and electrons should take place which probably accounts for the measured potential gradient in the shock front.

Shock width.—Measurements on the structure of the shock front in argon have been made at Cornell at a fore-pressure of 1 cm Hg. The point at which the onset of ionization occurs is determined by a conductivity measurement and the equilibrium region is specified by the luminosity. The Cornell measurements are in fair agreement with the computations here.²⁶ Additional measurements made by Laporte and his group at the University of Michigan on xenon, again at 1 cm Hg, also are in agreement with the present results in that there is a delay between the front of the shock and the region of luminosity and this delay decreases with increasing shock velocity.

Spectral distribution.—Observations on spectra in shock waves show that at low shock velocities distinct lines exist whereas at high shock velocities a continuous spectrum is seen. This is because of the following reasons. First, at low shock velocities, transitions from the

²⁵ T. G. Cowling, *Phil. Mag.* **33**, 61 (1942).

²⁶ Private communication from S. C. Lin to R. E. Duff.

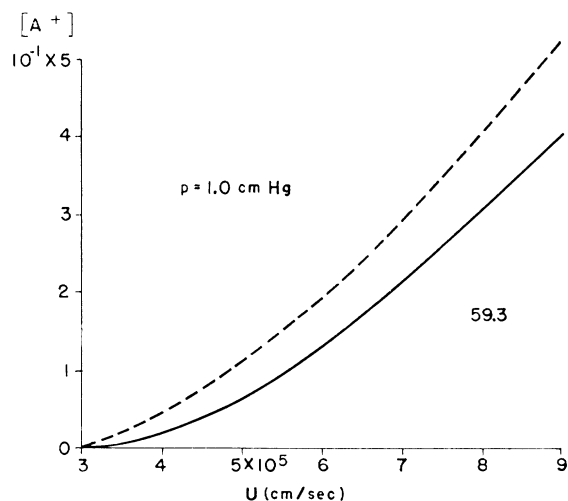


FIG. 9. Ionization vs shock velocity in the equilibrium region behind the shock front.

continuum to bound states do not occur because there are no free electrons, or at most, very few. There will, however, be many excited states of the atoms, thus one would expect a discrete spectrum to be observed.

For a high shock velocity and, consequently, a high degree of ionization, there are many electrons in free states. Since for the range of energies considered in this report these free states are in approximate Maxwellian distributions with energies centered between one and three electron volts, one would expect the radiated energy to be continuously distributed. This is the ordinary recombination spectrum which is observed in strong shocks.

In addition to the continuous recombination spectrum, one might expect to observe line spectra because of the presence of excited atoms. However, the pressure and temperature behind the shock front are high enough so that Stark, collision, and Doppler line broadening are significant. Undoubtedly most of the broadening of the spectral lines is due to the Stark effect which enters both because of the presence of ions and because of the high electric field in the shock front. This latter, which

has been mentioned previously (see end of Sec. 4 and under *Electric effects* of the present section), depends directly upon the electron density. These effects tend to smear the spectral lines out to such an extent that they are masked by the continuous recombination spectrum. Also, even when the degree of ionization is high, the occupation number for a particular excited state is relatively low and hence the line it emits is weak and more easily merges with the continuous background. Finally, there are many closely spaced lines in the argon spectrum and because of the broadening of the lines they may be expected to overlap. As the initial pressure is lowered, however, the spectral lines do begin to stand out against the continuous background. This is evident since for constant initial temperature the pressure behind the shock front decreases proportionately with decreasing fore-pressure. Consequently, the degree of ionization is higher and the temperature behind the shock front lower (see Fig. 9) and, although the higher degree of ionization will produce a relative increase in the amount of continuous radiation, the lower temperature and particularly the lower density will decrease the amount of line broadening. This is discussed more fully elsewhere.⁹

Luminosity.—As discussed previously, because of the smaller number of degrees of freedom available in a monatomic gas compared to a diatomic gas, much of the energy can go directly into ionization. Thus a relatively high degree of ionization can be obtained behind a shock front in an inert gas. Consequently, an argon shock of sufficiently high strength may be brilliantly luminous, and because of the continuous distribution of energy in the spectrum, it is used in experiments where such an energy distribution is desirable, e.g., in flash photography.²⁷

Note added in proof.—The theory and computations presented in this report are in general agreement with the work of Petschek²⁸ in which the effect of a lower electron temperature is discussed in some detail.

²⁷ Hamilton, Jensen, and Koski, Los Alamos Report 621 (unpublished).

²⁸ H. Petschek, thesis, Cornell University, 1955 (unpublished).